

Article

Study of the Effect of Seepage–Cyclic Load Coupling Disturbance on the Physical Field in Old Urban Underground Spaces

Jinghu Yang ^{1,2}, Ye Cheng ^{1,2,*}, Dawei Cui ^{1,2}, Zewei Zhang ^{1,2}, Bo Zhang ^{1,2} and Yixiong Gan ^{1,2}

¹ Research Institute of Emergency Science, Chinese Institute of Coal Science (CICS), Beijing 100013, China; yjh_cumtb@126.com (J.Y.); cuidawei@mail.ccrc.cteg.cn (D.C.); zhangzew16@tsinghua.org.cn (Z.Z.); zhangbo@mail.ccrc.cteg.cn (B.Z.); ganyixiong@mail.ccrc.cteg.cn (Y.G.)

² China Coal Technology & Engineering Group (CCTEG), Beijing 100013, China

* Correspondence: chengye@mail.ccrc.cteg.cn

Abstract: The safety and sustainability of urban underground spaces have become crucial considerations in development projects. Seepage and cyclic loads are the principal reasons for the instability and failure of old underground space structures. This study investigates the variations in physical fields of underground spaces in cities under the coupling disturbance of seepage and cyclic loads, focusing on underground civil air defense engineering in Beijing as a case study. Different seepage conditions and the effects of seepage–cyclic load coupling were simulated using the numerical calculation software Plaxis 3D V20. The results show that change in groundwater can affect the deformation of underground space, and the severity is related to the quantity and intersection state of tunnels, the location of rivers above, and the strength of materials. The coupling effect of seepage–cyclic load on urban underground space structures is more serious than that of a single percolation. Decrease in material strength and high traffic loads are the principal reasons for the failure of underground structures. A 30% decrease in material strength causes the displacement to increase almost 1.5 times, and maximum displacement under different traffic loads can vary by 3 times. This study holds significant implications for the design, maintenance, and engineering management of underground spaces, emphasizing the importance of sustainable practices in urban development and infrastructure.

Keywords: old urban underground space; seepage–cyclic load; sustainability; structural stability

Citation: Yang, J.; Cheng, Y.; Cui, D.; Zhang, Z.; Zhang, B.; Gan, Y. Study of the Effect of Seepage–Cyclic Load Coupling Disturbance on the Physical Field in Old Urban Underground Spaces. *Sustainability* **2024**, *16*, 3588. <https://doi.org/10.3390/su16093588>

Academic Editors: Martina Inmaculada Álvarez Fernández and Víctor Martínez-Ibáñez

Received: 4 March 2024

Revised: 15 April 2024

Accepted: 18 April 2024

Published: 24 April 2024



Copyright: © 2024 by the authors. Licensee MDPI, Basel, Switzerland. This article is an open access article distributed under the terms and conditions of the Creative Commons Attribution (CC BY) license (<https://creativecommons.org/licenses/by/4.0/>).

1. Introduction

Urban underground space refers to the building space below urban development, including urban underground shelters, underground spaces, underground parking lots, and so on. Many of these underground spaces are aging and suffer from neglect and lack of maintenance. Moreover, the cyclic dynamic load from vehicles above ground poses a serious threat, often resulting in ground collapsing, endangering lives and property. [1–4].

The safety of old urban underground space and the prevention of ground collapse have become major livelihood and development projects and have been highly valued by various countries [5–7]. In light of the imperative for sustainable development, it is crucial to underscore the significance of adopting sustainable practices in the management and rehabilitation of old urban underground spaces. Identifying the physical field variations law of old urban underground spaces and correctly understanding the mechanisms are of great significance for the design and repair of old urban underground spaces.

The instability and failure of underground space structures can be attributed to factors such as seepage and cyclic load. Seepage-related damage includes soil piping and falls in water level. Several studies have investigated these phenomena and have revealed

the impact on subsurface structures. For instance, Song [8] studied the seepage effect on soil arching in a shield tunnel and proposed that seepage leads to an increase in effective vertical stress and weakens the soil arching effect. Attard [9] studied the influence of underground structures on groundwater temperature and showed that underground structures and groundwater interact with each other. Di [10] evaluated hydraulic head distribution in front of a shield tunnel in a saturated soil layer, and relative theoretical analysis and numerical simulations were carried out. The study revealed dynamic changes in the permeability field and provided important hydrogeological information to help prevent and control water-related problems in underground structures. By using the equivalent continuum model, Sheng [11] conducted studies on the seepage and mechanical characteristics and carried out coupling calculations on the seepage field and stress field of the underground powerhouse caverns of Xiluodu Hydropower Station. The study illustrated the importance of the interaction of water flow and stress fields and proposed that the coupled effects of infiltration and stress in geotechnical engineering practice should be considered.

The impact of traffic cyclic load on underground spaces primarily manifests in four key aspects: vertical pressure, horizontal force, the influence of long-term cyclic load, and shock effects [12–16]. Daehyeon [17] utilized the finite element software ABQUS to investigate the dynamic response of a single tire on the road surface and provided valuable insights into the interaction between the tire and road surface. Saad [18] used the finite element software ADINA to model subgrade of different materials and made a comparative analysis of the maximum compressive strain at the top and maximum tensile strain at the bottom of the subgrade at a speed of 50 km/h. This provided a reference for studying the influence of different roadbed materials on vehicle running. Additionally, Wu [19] regarded vehicle-mounted vehicles as non-uniformly distributed moving loads. By establishing a three-dimensional transient dynamic finite element model, time-history variation rules and spatial distribution rules of road dynamic response under moving loads were analyzed, which provided a comprehensive perspective for vehicle motion characteristics under different road conditions.

In July 2023, Beijing experienced an exceptionally heavy rainstorm. Changes in groundwater and traffic loads have a significant effect on underground structures. As an important form of underground space, civil air defense engineering develops the important functions of a wartime air defense command center, communication center, hiding place, and so on. However, civil air defense structures are predominantly underground, rendering them vulnerable to the impacts of both traffic load and groundwater fluctuations and presenting intricate challenges to their structural integrity and stability. Currently, many civil air defense tunnels have incurred extensive damage, necessitating significant costs for repair and maintenance. According to related surveys, most civil air defense tunnels have not yet reached the overall fatigue resistance of the structure when damaged.

Many researchers have investigated and analyzed this phenomenon and found that there are many reasons for early damage in civil air defense engineering, among which some of the principal reasons are seepage and cyclic loads [20–23]. The current research mainly focuses on seepage and traffic loads and roads, as well as the effect of speed on road surfaces [24–27]. As structures situated underground, significant damage to civil air defense tunnels can lead to ground subsidence [28,29]. Li [30] summarized research on the dynamic characteristics and constitutive models of soil under long-term cyclic loads and pointed out that long-term vibration loads have a significant impact on the performance of geotechnical engineering structures. Cao [31] provided an analytical solution to study the impact of surface moving loads on underground tunnels, which is used to calculate the vibration generated by moving loads above circular tunnels.

Despite the known impacts of seepage and cyclic loads, the coupling effects of these factors on the physical field of old civil air defense engineering remain poorly understood. Current studies about civil air defense engineering do not consider the coupling

disturbance of seepage and traffic cyclic loads, and the effect of seepage–traffic cyclic loads on old civil air defense engineering has not been mentioned. Therefore, this paper mainly focuses on the physical field of seepage–cyclic load coupling disturbance on civil air defense structures, providing a theoretical basis for the safe operation and maintenance of cities.

In this paper, the effect of seepage–cyclic load coupling disturbance on the physical field of old civil air defense engineering was studied. Firstly, from a case study of underground civil air defense engineering in Beijing, the primary size and burial depth of the tunnels was determined through field visits and investigations. Then, leveraging this information, the finite element software Plaxis 3D was used to simulate alterations in the physical field of the underground space under varying groundwater seepage conditions. Subsequently, dynamic responses of the underground space were calculated, taking into account the coupling effect of seepage and cyclic loads. The effect factors, such as the quantity and intersection state of tunnels, the location of rivers, and the rate of water table decline were investigated as well. This study can provide a sustainability development basis for the design, maintenance, and engineering management of underground spaces, which can enhance the resilience and longevity of underground structures.

2. Engineering Background

2.1. Project Overview

This study uses old underground civil air defense engineering in Beijing as a representative case. According to the field visit and observation, civil air defense tunnels are categorized into two types, Type A and Type B, as shown in Figure 1a. Type A tunnels have a span of 3 m and a side wall height of 3 m, with arch radii of 1.5 m. Type B tunnels have a span of 1.5 m and a side wall height of 2 m, with arch radii of 0.75 m. These tunnels are typically buried at a depth of 8 m underground and are surrounded by rivers and roads. The depth of the river is generally 3 m; the width of the river bottom is 3 m; and the width of the river surface is 6 m, as shown in Figure 1b. The road width is 13 m, and the thickness of the road surface is negligible, as shown in Figure 1c. Observation found that tunnel layouts often consist of one to four tunnels arranged side by side, with instances of tunnels intersecting each other. Some tunnels are situated close to rivers, with the nearest tunnel located less than 10 m horizontally from a river.

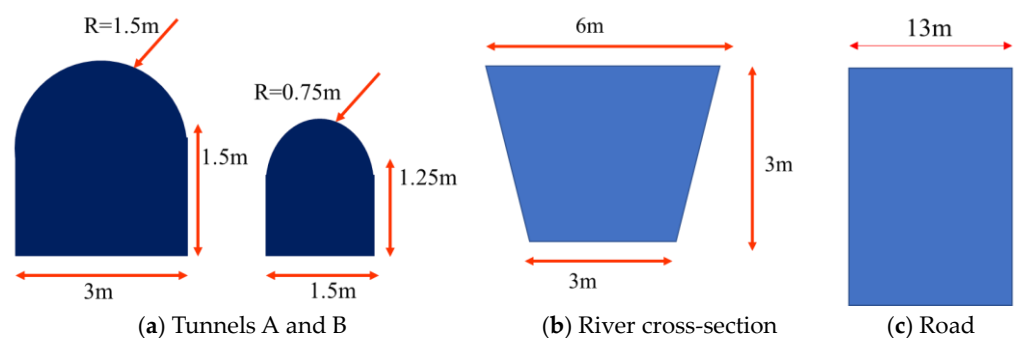


Figure 1. Project overview.

2.2. Engineering Geology and Hydrogeological Conditions

(1) Geotechnical characteristics

Considering the geological conditions of Beijing, the surrounding geological environment of the underground civil air defense tunnels was investigated. It was determined that clay and sandy soil are the primary soil layers in this region. Subsequently, soil mechanics tests were conducted on these two layers of soil, and their physical parameters were determined, as listed in Table 1.

(2) Hydrogeological conditions

According to data released by the Beijing water authority [32], the lowest water level in Beijing typically occurs around May to June, while the highest water level is recorded in December. In 2023, the highest groundwater level was approximately 15 m underground, while the lowest groundwater level was 18 m underground, as shown in Figure 2. In July 2023, an extremely heavy rainstorm occurred in Beijing, hence the urban groundwater level was significantly higher than in previous years. The water level data considered in this study relate to an unconfined aquifer, also known as a water table aquifer. In an unconfined aquifer, the upper boundary is not an impermeable layer, which means that fluctuations in water level are primarily influenced by factors such as precipitation, surface water recharge, and human activities, including the extraction of groundwater.

Table 1. Soil Layer Parameters.

Parameters	Clay	Sandy
Thickness (m)	6	20
Density (g/cm ³)	1.92	1.92
Saturation density (g/cm ³)	1.973	2.047
Natural moisture content (%)	24.2	15.4
Cohesive force (kPa)	26.4	24.1
Internal friction angle (°)	26.24	34.37
Elastic modulus (MPa)	4×10^4	4×10^4

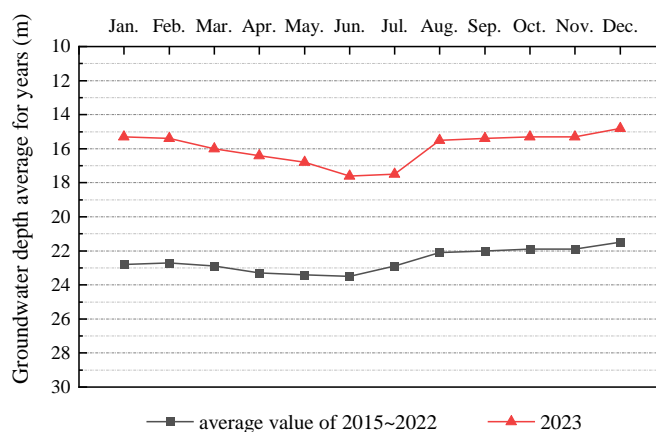


Figure 2. Groundwater level in Beijing [30].

3. Numerical Calculation

3.1. Plaxis 3D

The actual conditions were simulated using Plaxis 3D numerical calculation software. Plaxis 3D is a finite element software developed in the Netherlands for professional geotechnical engineering. It has strong applicability and can simulate complex geological engineering conditions, and it is especially suitable for deformation and stability analysis. It can analyze deformation, consolidation, graded loading, stability analysis, seepage calculation, and the influence of low-frequency dynamic loads can also be considered. The operating interface is user-friendly.

3.2. Seepage Finite Element Calculation of Underground Civil Air Defense Tunnels

(1) Case arrangement

The variation in urban groundwater level presents obvious seasonal characteristics. During the rainy season, groundwater level will rise, and it will decrease in the dry season. The sudden rise and fall of the groundwater level will cause significant changes in the effective stress of the soil, which will affect the soil around civil air defense engineering

works. In order to study the seepage effect, in this section, the influence of tunnel type, tunnel arrangement, intersection of tunnels, and change of groundwater level on the civil air defense tunnels under the river is considered.

The cases are listed in Table 2. Cases 1–4 relate to the influence of the quantity of tunnels, cases 5–8 relate to the increase in number of intersections of tunnels, cases 9–11 relate to the influence of the location of the river, and cases 12–13 relate to the decrease in strength of tunnel materials. In the River column, lack of an entry means the river does not exist in the corresponding model. In the selection of material strength data, the 70% value represents a condition where the material is under a moderate level of stress, which is common in many engineering situations. On the other hand, the 40% value represents a lower stress level, which is relevant to material degradation and aging. The various case stereograms are shown in Figure 3.

In the Plaxis model, in order to avoid boundary effects, the model size is set as $x_{\min} = -50$ m, $x_{\max} = 50$ m, $y_{\min} = 0$, $y_{\max} = 50$ m. In the seepage calculation, the boundary condition of x and y is set as normally fixed. The bottom surface of the model is full-fixed, and the top surface is free. The material model adopts the Mohr–Coulomb law, and the type is drainage. The model adopts the Van Genuchten model. In the calculation of cyclic loads, the boundary condition of x and y is viscous. The bottom surface is full-fixed, and the top surface is free.

Table 2. Calculation cases under seepage conditions.

Case	Quantity of Y-Direction Tunnels	Quantity of X-Direction Tunnels	Horizontal Distance from River	Material Strength
1	1	/	/	100%
2	2	/	/	100%
3	3	/	/	100%
4	4	/	/	100%
5	2	1	/	100%
6	2	2	/	100%
7	2	3	/	100%
8	2	4	/	100%
9	1	/	0	100%
10	1	/	6	100%
11	1	/	/	70%
12	1	/	/	40%

(2) Calculation phase settings

The change in groundwater level can be categorized into multiple stages. When the rainy season ends or groundwater is pumped in large quantities, the water level will decrease. Therefore, two calculation phases were set: (1) sudden drawdown of groundwater; (2) slow drawdown of groundwater. The highest water level is 15 m underground, and the lowest water level is 18 m underground. During the sudden drawdown phase, the water level falls at a rate of 0.8 m/day, whereas during the slow drawdown phase, the rate reduces to 0.1 m/day. The process for the calculation phases is depicted in Figure 4.

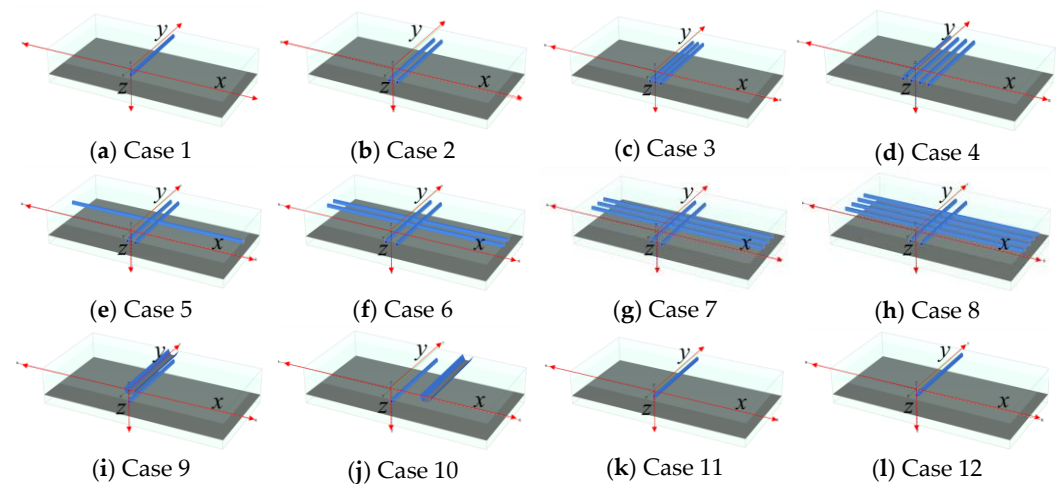


Figure 3. Seepage calculation cases.

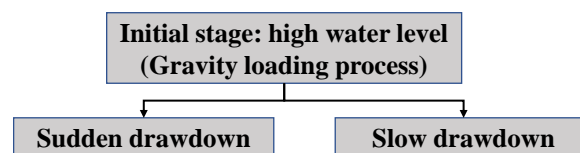


Figure 4. Seepage calculation phase process.

3.3. Seepage–Traffic Load Coupling Disturbance Calculation

On the basis of the seepage calculation, this section applies traffic loads to calculate the displacement under the coupling effect of seepage–traffic cycle loads.

(1) Traffic cycle loads

Due to the vibration of the vehicle and the unevenness of the road surface during driving, the load will be applied on the road surface in the form of waves [33,34]. Since the sinusoidal load model is both practical and representative of actual engineering conditions, it is commonly employed by scholars to simulate vehicle loads [35,36]. The load can be described as

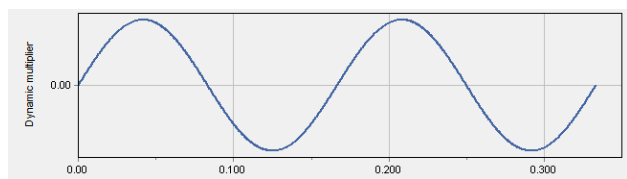
$$F(t) = P_0 + P \sin(\omega t) \quad (1)$$

in which P_0 is the vehicle static load (20 kN for small cars and 100 kN for large cars); ω is the vibration frequency of the vehicle load ($\omega = 2\pi v/L$); v is the driving speed; L is the car length, referring to JTGB 01-2014 Highway Engineering Technical Standard [37], where L is 6 m; P is the amplitude of vehicle load, where $P = M_0 \alpha \omega^2$, $M_0 = 120 \text{ N}\cdot\text{s}^2/\text{m}$, $\alpha = 2 \text{ m}$.

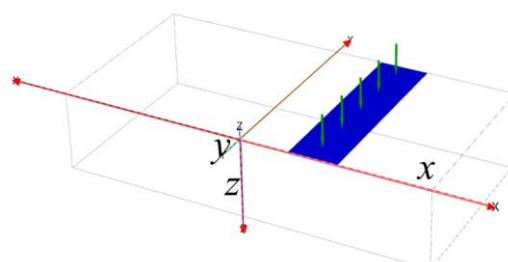
Based on the actual driving characteristics of the vehicle, three vehicle speeds were considered: 20 km/h, 60 km/h, 100 km/h, namely F_1 , F_2 , F_3 . Table 3 lists the relationship between vehicle speed and parameters of the sinusoidal load model. The dynamic multiplier is shown in Figure 5a, and the cycle load is shown in Figure 5b.

Table 3. Relationship between vehicle speed and parameters.

Load Type	Speed of Vehicle v (km/h)	Frequency ω (Hz)	Amplitude P (kN)	Static Load P_0 (kN)
F_1	20	6	9	100
F_2	60	17	69	100
F_3	100	29	202	100



(a) Dynamic multiplier



(b) Cyclic load

Figure 5. Dynamic multiplier and cyclic load.

(2) Case setting

On the basis of the seepage calculation, various factors were considered, including tunnel type, quantity of tunnels, tunnel intersections, distance from the river, and changes in material parameters. The cases are listed in Table 4. The various case stereograms are shown in Figure 6.

Table 4. Calculation cases under Seepage–Traffic load coupling disturbance calculations

Case	Y-Direction Tunnels	X-Direction	Horizontal Distance from River	Material Strength
13	1	/	/	100%
14	4	/	/	100%
15	1	/	0	100%
16	1	/	5	100%
17	2	1	/	100%
18	2	4	/	100%
19	2	/	/	70%
20	2	/	/	40%

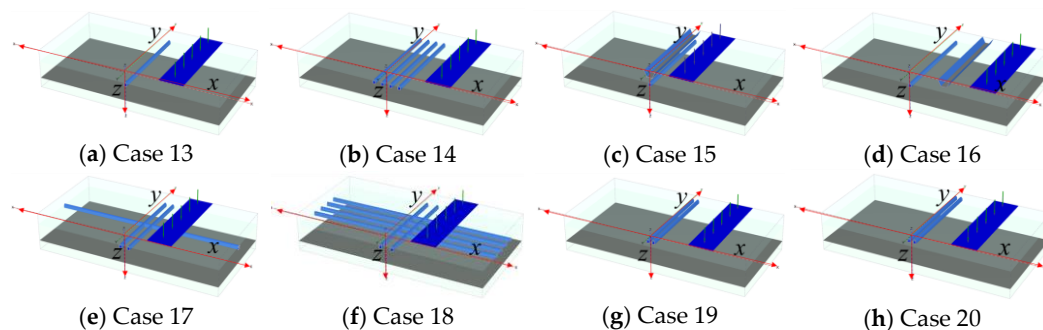


Figure 6. Calculation cases.

(3) Calculation phase settings

Based on the seepage calculation, the impact of traffic loads was calculated. The action time of traffic loads was set as 36,000 s. Each model was calculated under different load frequencies, as shown in Figure 7.

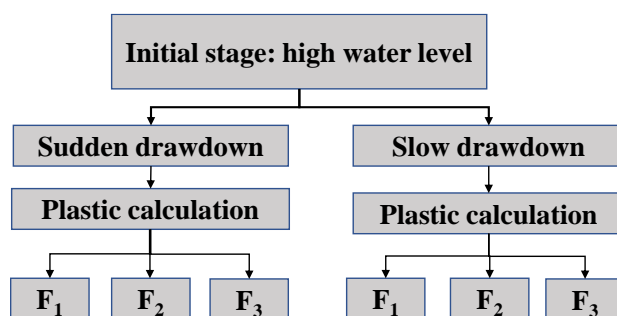


Figure 7. Seepage–Traffic load coupling disturbance calculation phase process.

4. Analysis of Calculation Results

According to the above cases, the calculation is divided into two stages. The first stage is to calculate the impact of seepage on civil air defense engineering. In the second stage, the displacement changes of civil air defense tunnels are considered after accounting for both traffic loads and seepage effects.

4.1. The Seepage Calculation of Old Civil Air Defense Engineering

The overall displacement of tunnel A under sudden drawdown and slow drawdown of groundwater level is shown in Figures 8 and 9. In Figures 8 and 9, it is evident that there are significant changes in displacement. According to the field visit and observation, it was found that certain ground settlement had occurred. The calculation results of the model are consistent with the observed trend, including the performance data of existing tunnels and the amount of ground settlement. This indicates that the calculation of this model is reasonable.

The displacement of the ground center point under different conditions is presented in Figure 10. In Figure 10, it can be seen that the ground displacement caused by sudden drawdown of groundwater is always higher than that caused by slow drawdown. With respect to the quantity of tunnels, as the quantity of tunnels increases, the ground displacement increases after groundwater changes. With respect to the intersection of tunnels, it can be seen that as the quantity of tunnel intersections increases, the ground displacement also increases. Regarding the location of rivers, the smaller the horizontal distance of the tunnel from the river, the greater the displacement of the tunnel chamber and its surroundings. Regarding groundwater level changes, the presence of rivers leads to significant infiltration effects around the tunnels, and the impact of groundwater level changes is weakened. With respect to the material strength changes, under the seepage effect, the lower the material strength, the higher the ground displacement. Regarding the type of tunnel, the ground displacement of tunnel B under seepage is smaller than that of tunnel A.

To express the influence of factors on surface displacements clearly, based on the above results, the relationships between the influencing factors and surface displacements are summarized in Table 5.

Table 5. The changes in surface displacement under seepage calculations.

No.	Factors	Changes in Factors	Changes in Displacement
1	Rate of groundwater drawdown	↑	↑
2	Quantity of tunnels	↑	↑
3	Quantity of tunnel intersections	↑	↑
4	Horizontal distance from the river	↓	↑
5	Material strength	↓	↑
6	Cross-sectional area of tunnels	↑	↑

When the water level drops rapidly, the force balance of the soil layer will be disrupted, and the effective stress changes rapidly, causing the ground to sink, which is detrimental to the civil air defense tunnel. When the quantity of tunnels increases, the underground space increases and support decreases, making it more likely to cause ground collapse, which is also detrimental to the structure. Similarly, an increase in tunnel intersections diminishes the stiffness of the intersection area, exacerbating tunnel and surface displacement under seepage effects, thus affecting structural stability. With the seepage effect, the displacement of the tunnel and surface is greater than that of a single tunnel intersection. When there is a river near the tunnels, the seepage effect of the river is significant, and the impact of groundwater changes will be weakened. Furthermore, when tunnel material strength decreases, the ground displacement caused by seepage is the greatest, indicating that the decrease in material strength under seepage has a significant impact on ground displacement, far worse than the impact of tunnel layout, and is the most detrimental for civil air defense tunnels.

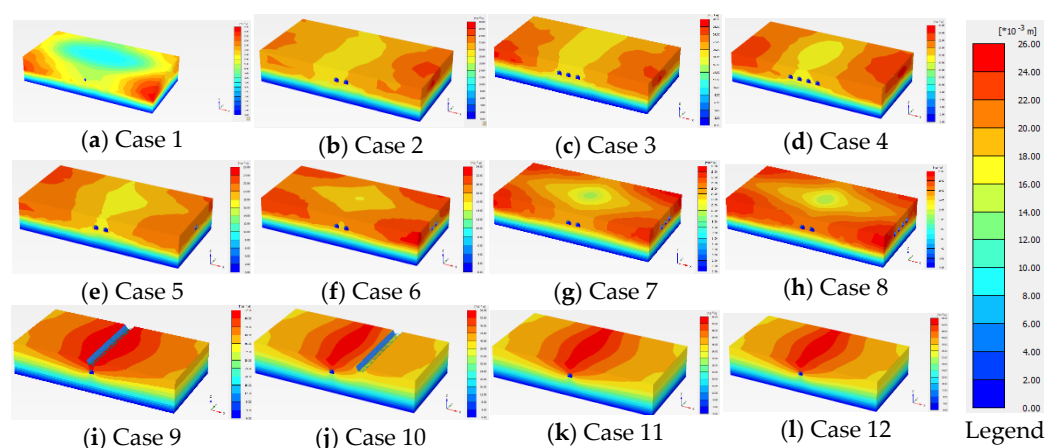


Figure 8. Displacement diagram of tunnel A under sudden drawdown.

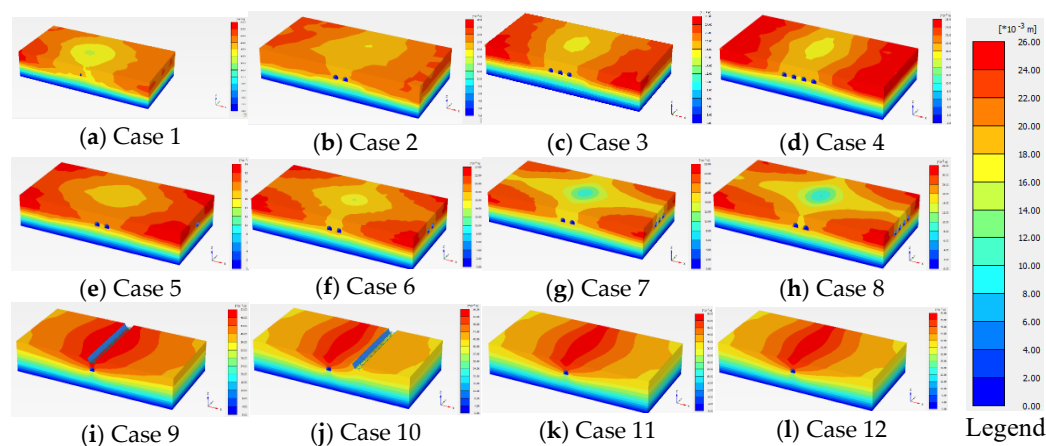


Figure 9. Displacement diagram of tunnel A under slow drawdown.

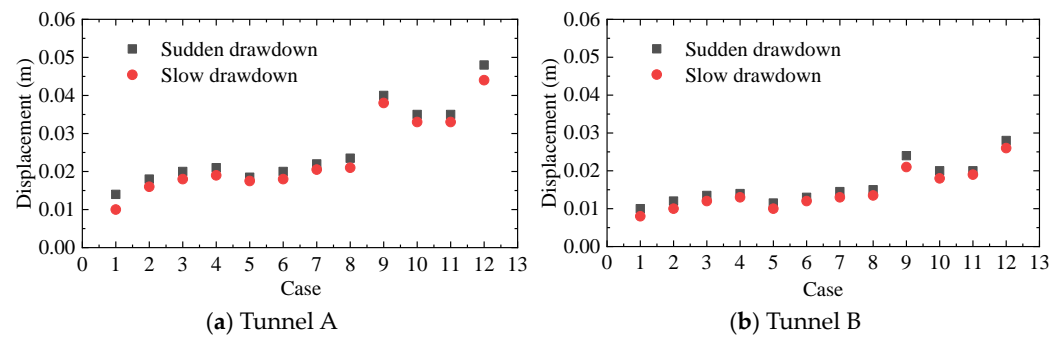


Figure 10. Ground displacement under seepage.

Based on a comprehensive analysis, the weakening of the material strength of the tunnel is most sensitive to the effect of seepage, and displacement of the ground is the largest. In practical engineering, special attention should be paid to old civil air defense tunnels to avoid accidents such as collapse caused by groundwater or river seepage.

4.2. Finite Element Calculation of Seepage–Cyclic Load Coupling Disturbance

It has been verified in cases 1–12 that tunnel type A is more easily affected than tunnel type B, so studies on tunnel type A were conducted in cases 13–20. The displacement of tunnel A was calculated separately under sudden drawdown and slow drawdown of groundwater. F_i ($i = 1, 2, 3$) represents different frequencies and magnitudes of cyclic load. X_i ($i = 1, 2, 3, 4$) represents the roof displacement of different tunnels, with a larger i indicating that the tunnels are closer to the road surface, 1 representing the farthest and 4 representing the nearest. It should be noted that the displacements in the figures refer to the roof displacement of the tunnel central section point. The results of cases 13–20 are shown in Figures 11–16. The calculation results of the model are consistent with the observed trend. This indicates that the calculation of this model is reasonable.

Figure 11 shows the roof displacement of a single tunnel under the action of F_3 . It can be seen that the roof displacement is larger when the groundwater level drops sharply. As the frequency of the cyclic load increases, the displacement increases. The result for a parallel arrangement of tunnels is shown in Figure 12. It can be seen that as the quantity of tunnels increases, the larger the roof displacement of the tunnels. Compared to the sudden drawdown of groundwater, the impact of traffic loads is relatively small under slow drawdown groundwater. As the frequency of action increases, the displacement increases.

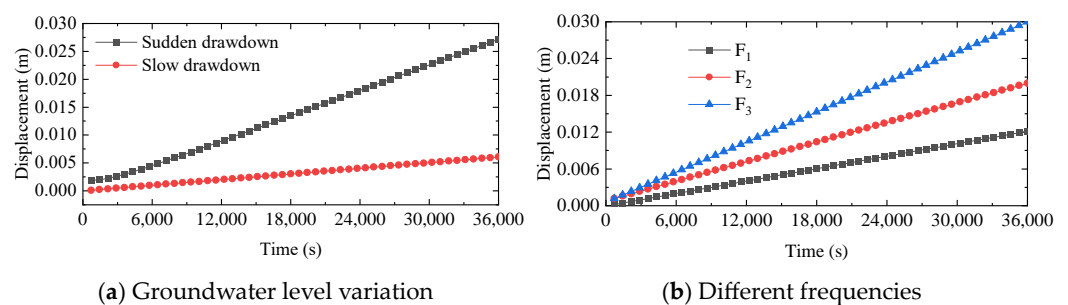


Figure 11. The roof displacement results of Case 13.

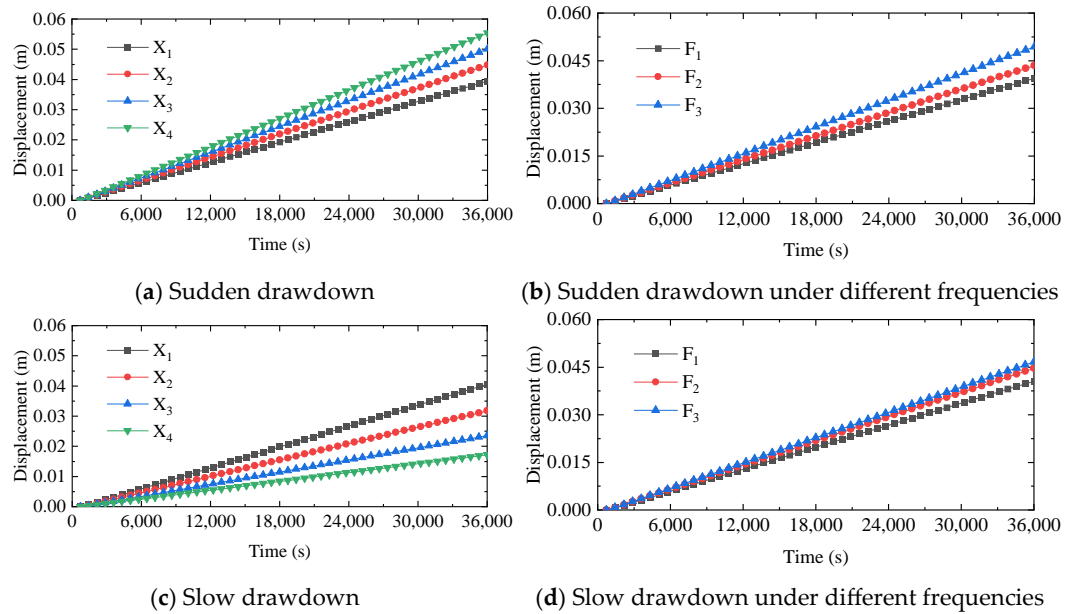


Figure 12. The roof displacement results of Case 14.

With respect to tunnel intersections, the roof displacements of the tunnel are shown in Figures 13 and 14. It can be seen that the displacement of the tunnel is higher than that for the parallel arrangement of the tunnels under the same load. Similarly, for sudden drawdown of groundwater, the displacement is higher than that for slow drawdown.

Figures 15 and 16 show the coupling effect of seepage and traffic load when the river is located near the tunnel. It can be seen that, when the river is directly located above the tunnel roof, using the same frequency of loading, the roof displacement of the tunnel is higher than that in other cases. This indicates that the river has an adverse effect on the civil air defense tunnel. The difference between the frequencies of each action is relatively small, so the influence of rivers is the dominant factor.

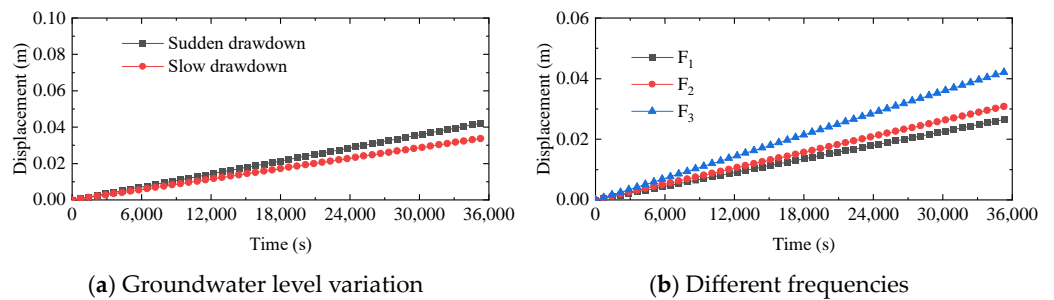


Figure 13. The roof displacement results of Case 15.

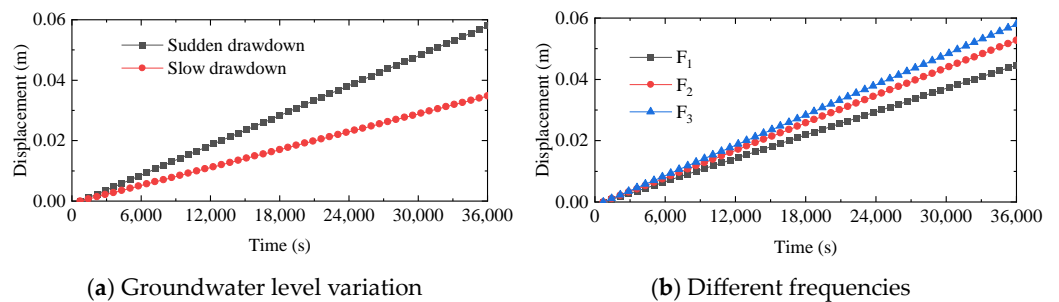


Figure 14. The roof displacement results of Case 16.

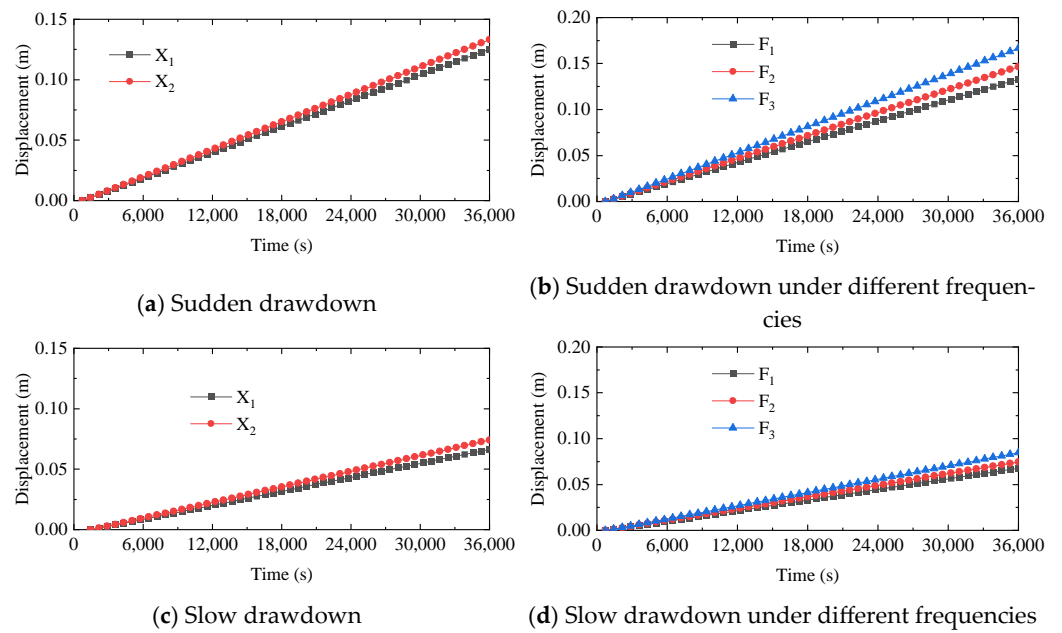


Figure 15. The roof displacement results of Case 17.

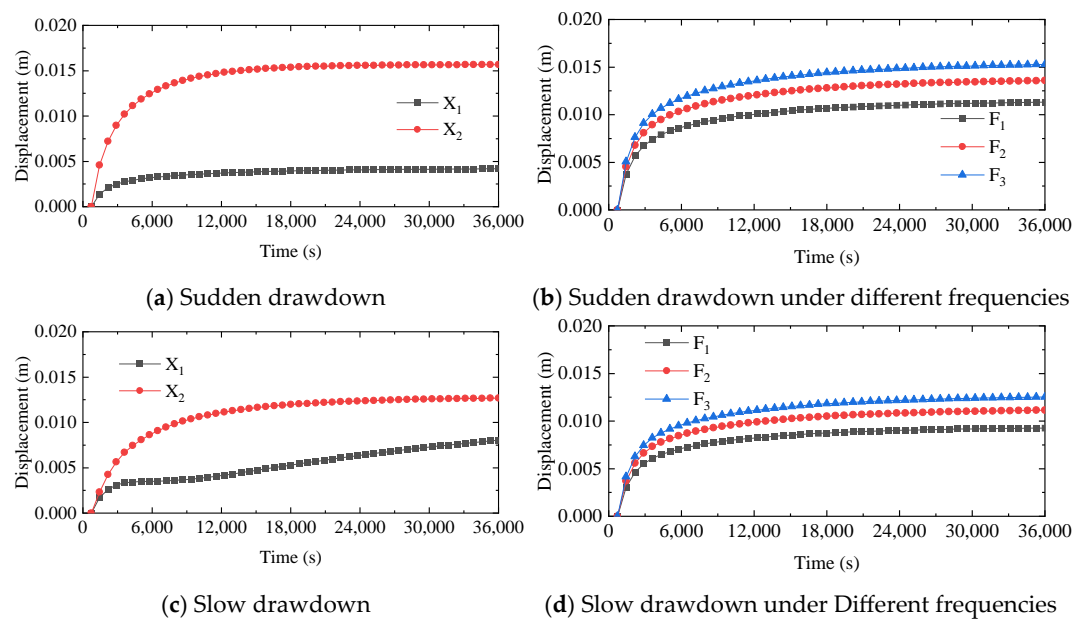


Figure 16. The roof displacement results of Case 18.

Figures 17 and 18 show the coupling effect of seepage and traffic load when the material parameters change. In Figures 17 and 18, it can be seen that as the material strength decreases, the larger the decrease in material strength and the larger the roof displacement of the tunnel at the same loading frequency. As the frequency of loading increases, the roof displacement of the tunnel gradually increases and is far worse than in the other cases. When the material strength decreases, the tunnel will be in a very unfavorable state under the coupling effect of seepage and load.

In order to express the displacement effect of factors clearly, based on the above results, the relationships between the influencing factors and displacements are summarized in Table 6.

Table 6. The changes in surface displacement under Seepage–Traffic load coupling disturbance calculations

No.	Factors	Changes in Factors	Changes in Displacement
1	Rate of groundwater drawdown	↑	↑
2	Frequency of cyclic load	↑	↑
3	Quantity of tunnel intersections	↑	↑
4	Horizontal distance from the cyclic load	↓	↑
5	Horizontal distance from the river	↓	↑
6	Material strength	↓	↑

Changes in groundwater can induce displacement in civil air defense engineering structures. Sudden fluctuations in groundwater levels can significantly impact civil air defense structures through seepage effects. When coupled with traffic loads, underground tunnels may sustain damage, potentially leading to surface collapse. The reduction in tunnel strength can exacerbate roof displacement within the tunnel. Given that the strength of tunnel materials tends to decrease over time in old urban underground spaces, this issue warrants considerable attention.

The results of this study indicate the detrimental effects of vehicular dynamic loads on underground space structures. They illustrate that higher vehicle speeds correspond to increased vibration intensity, exacerbating the structural impact on underground spaces. Therefore, it is necessary to focus on the underground space in areas with fast vehicle speeds and areas where there are rivers. Regarding the problem of decreased strength of underground space structural materials, timely support and reinforcement operations are needed to avoid damage to underground space structures under seepage–traffic cyclic load coupling disturbance.

The above finding can provide a basis for evaluating the status of old underground spaces. Based on identified underground water and the local geological environment, it is possible to monitor the surroundings of old underground space structures. In addition, according to the potential impacts on older urban underground spaces, designers can make more scientific choices in the siting, design, and construction of new projects.

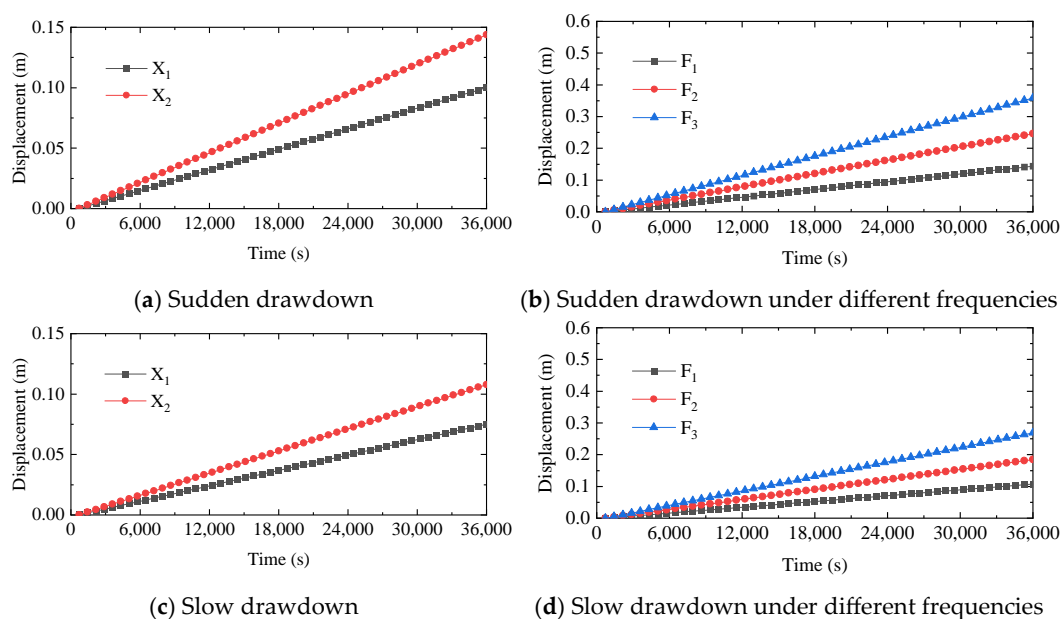


Figure 17. The roof displacement results of Case 19.

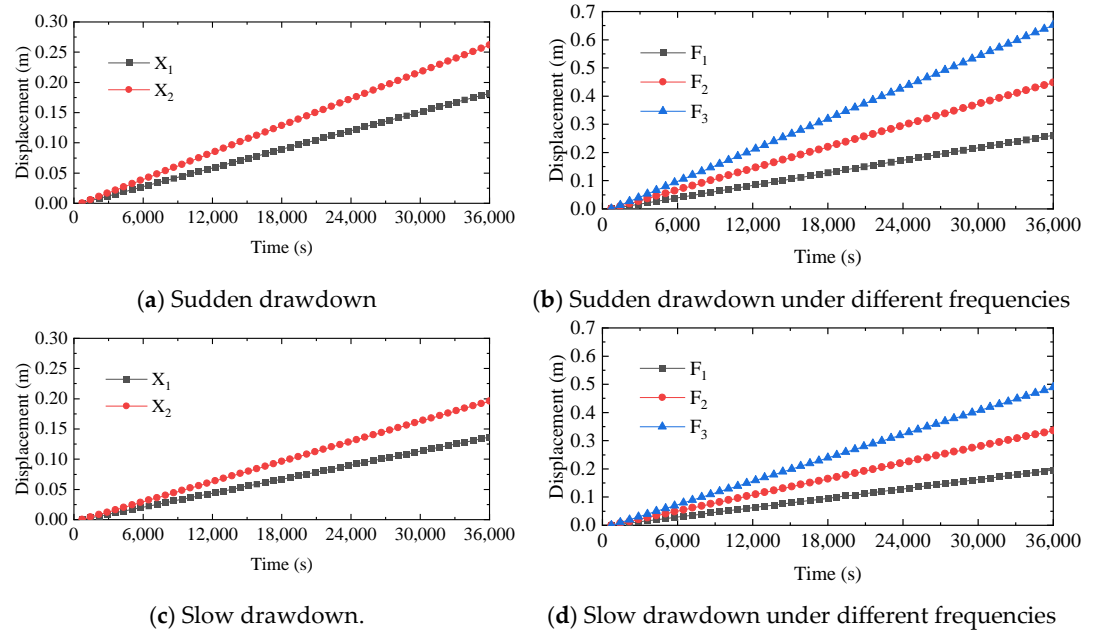


Figure 18. The roof displacement results of Case 20.

5. Conclusions

The effect of seepage–cyclic load coupling disturbance on the physical field was studied in this paper with respect to the collapse of old urban underground spaces. Based on extensive analysis, the primary conclusions are as follows:

(1) From the field visit and observation, the primary types of civil defense tunnels in the Beijing area can be categorized into two types. Based on geological conditions and burial depth, the effect of seepage–cyclic load coupling disturbance on the physical field in old urban underground spaces can be simulated using Plaxis 3D.

(2) Fluctuations in groundwater significantly affect underground space structures. The faster the groundwater level drops, the larger the ground displacement, which is detrimental to the structure. The more tunnels there are, the larger the ground displacement after the groundwater level changes. The more tunnels intersect, the larger the impact of seepage. The more the material strength decreases, the larger the impact of seepage and the greater the ground displacement. The larger the tunnel, the larger is the effect of seepage.

(3) The coupling effect of seepage and traffic load significantly influences tunnel roof displacement. Higher vehicle speeds and loading frequencies correlate with increased roof displacement, posing greater risks to structural stability. The variation in tunnel roof displacement is not only related to the variation in groundwater level, but also to the horizontal distance of the road: the closer to the road, the larger the displacement. The higher the decrease in the strength of underground structural materials, the higher the roof displacement of the tunnel, so it is easy for ground collapse to be caused under external loads. A 30% decrease in material strength can result in an approximately 1.5 times increase in displacement, with maximum displacement under different traffic loads varying by up to 3 times.

In engineering applications, special attention should be given to the condition of old urban underground spaces when the groundwater declines rapidly. Underground structures near traffic loads and rivers require particular monitoring to ensure safety. For newly constructed underground structures, it is advisable to avoid proximity to main roads and rivers above ground. These findings offer direct implications for engineering and construction practices in Beijing and other urban areas with similar geological and infrastructural conditions.

Author Contributions: Conceptualization, J.Y.; methodology, J.Y. and Y.C.; project administration, J.Y.; software, B.Z.; supervision, Y.C.; visualization, J.Y. and Z.Z.; writing—original draft, J.Y. and Y.C.; writing—review and editing, D.C. and Y.G.; funding acquisition, J.Y. All authors have read and agreed to the published version of the manuscript.

Funding: This research was funded by the Innovation and Entrepreneurship Science and Technology Project of China Coal Technology and Engineering Group (No. 2022-2-MS003).

Institutional Review Board Statement: Not applicable.

Informed Consent Statement: Not applicable.

Data Availability Statement: The data that support the findings of this study are available from the corresponding author upon reasonable request.

Conflicts of Interest: The authors declare no conflicts of interest.

References

- Zheng, D.; Tang, L.; Wang, Y.; Sun, Y. Dynamic stress accumulation effects on soil strength under cyclic loading. *Soils Found.* **2022**, *62*, 101164. <https://doi.org/10.1016/j.sandf.2022.101164>.
- Gu, C.; Hu, L.; Zhang, X.; Wang, X.; Guo, J. Climate change and urbanization in the Yangtze River Delta. *Habitat Int.* **2011**, *35*, 544–552.
- Kontokosta, C.E.; Malik, A. The resilience to emergencies and disasters index: Applying big data to benchmark and validate neighborhood resilience capacity. *Sustain. Cities Soc.* **2018**, *36*, 272–285.
- Tan, F.; Tan, W.; Yan, F.; Qi, X.; Li, Q.; Hong, Z. Model Test Analysis of Subsurface Cavity and Ground Collapse Due to Broken Pipe Leakage. *Appl. Sci.* **2022**, *12*, 13017. <https://doi.org/10.3390/app122413017>.
- Forero-Ortiz, E.; Martínez-Gomariz, E. Hazards threatening underground transport systems. *Nat. Hazards* **2020**, *100*, 1243–1261.
- Lyu, H.-M.; Zhou, W.-H.; Shen, S.-L.; Zhou, A.-N. Inundation risk assessment of metro system using AHP and TFN-AHP in Shenzhen. *Sustain. Cities Soc.* **2020**, *56*, 102103.
- Dai, Z.; Peng, L.; Qin, S. Experimental and numerical investigation on the mechanism of ground collapse induced by underground drainage pipe leakage. *Environ. Earth Sci.* **2023**, *83*, 32. <https://doi.org/10.1007/s12665-023-11344-w>.
- Song, X.; Meng, F.-Y.; Chen, R.-P.; Wang, H.-L.; Wu, H.-N. Effect of seepage on soil arching effect in deep shield tunnel. *Undergr. Space* **2023**, *12*, 218–233.
- Attard, G.; Rossier, Y.; Winiarski, T.; Eisenlohr, L. Deterministic modeling of the impact of underground structures on urban groundwater temperature. *Sci. Total Environ.* **2016**, *572*, 986–994.
- Di, Q.; Li, P.; Zhang, M.; Guo, C.; Wang, F.; Wu, J. Three-dimensional theoretical analysis of seepage field in front of shield tunnel face. *Undergr. Space* **2022**, *7*, 528–542.
- Jinchang, S. Review of Coupled Study on Seepage Stress in Fractured Rock Masses. *Rock Mech.* **1998**, *19*, 92–98 (In Chinese)
- Chen, F.; Wang, L.; Zhang, W. Reliability assessment on stability of tunnelling perpendicularly beneath an existing tunnel considering spatial variabilities of rock mass properties. *Tunn. Undergr. Space Technol.* **2019**, *88*, 276–289.
- Jiang, T.; He, T.; Liu, C.; Li, L. Soil deformation under cyclic horizontal load in sand: Insights from experiments. *J. Eng. Res.* **2023**. <https://doi.org/10.1016/j.jer.2023.12.010>.
- Li, P.; Wei, Y.; Zhang, M.; Huang, Q.; Wang, F. Influence of non-associated flow rule on passive face instability for shallow shield tunnels. *Tunn. Undergr. Space Technol.* **2022**, *119*, 104202.
- Pujades, E.; Jurado, A. Groundwater-related aspects during the development of deep excavations below the water table: A short review. *Undergr. Space* **2021**, *6*, 35–45.
- Xiang, Y.; Liu, H.; Zhang, W.; Chu, J.; Zhou, D.; Xiao, Y. Application of transparent soil model test and DEM simulation in study of tunnel failure mechanism. *Tunn. Undergr. Space Technol.* **2018**, *74*, 178–184.
- Kim, D.; Salgado, R.; Altschaeffl, A.G. Effects of supersingle tireloadings on pavements. *J. Transp. Eng.* **2005**, *131*, 732–743.
- Saad, B.; Mitri, H.; Poorooshasb, H. Three-dimension dynamic analysis of flexible conventional pavement foundation. *J. Transp. Eng.* **2005**, *131*, 460–469.
- Jinmin, W.; Xiaowei, F. Three dimensional non-uniform dynamic response analysis of rubber asphalt surface structure under heavy load. *Highway* **2018**, *63*, 15–20 (In Chinese)
- Xue, W.; Chen, S.; Wang, Q. Cyclic Loading Test Conducted on the Bottom Joints of a Hybrid Precast Utility Tunnel Composed of Double-Skin Sidewalls and a Precast Bottom Slab. *Buildings* **2024**, *14*, 341; <https://doi.org/10.3390/buildings14020341>
- Zhang, Z.; Zhou, C.; Remennikov, A.; Wu, T.; Lu, S.; Xia, Y. Dynamic response and safety control of civil air defense tunnel under excavation blasting of subway tunnel. *Tunn. Undergr. Space Technol.* **2021**, *112*, 103879 <https://doi.org/10.1016/j.tust.2021.103879>
- Sun, W.; Liang, Q.; Qin, S.; Yuan, Y.; Zhang, T. Evaluation of groundwater effects on tunnel engineering in loess. *Bull. Eng. Geol. Environ.* **2021**, *80*, 1947–1962. <https://doi.org/10.1007/s10064-020-02095-0>
- Liu, Y.; Zhang, Z.; Liu, Z.; Xue, J. The effects of undercrossing tunnelling on the settlement of footings subjected to cyclic loading. *Tunn. Undergr. Space Technol.* **2023**, *132*, 104792. <https://doi.org/10.1016/j.tust.2022.104792>

24. Tan, Y.; Jiang, W.; Luo, W.; Lu, Y.; Xu, C. Longitudinal sliding event during excavation of Feng-Qi station of Hangzhou metro line 1: Postfailure investigation. *J. Perform. Constr. Facil.* **2018**, *32*, 04018039.
25. Tan, Y.; Jiang, W.-Z.; Rui, H.-S.; Lu, Y.; Wang, D.-L. Forensic geotechnical analyses on the 2009 building-overturning accident in Shanghai, China: Beyond common recognitions. *J. Geotech. Geoenviron. Eng.* **2020**, *146*, 05020005
26. Ren, D.-J.; Shen, S.-L.; Cheng, W.-C.; Zhang, N.; Wang, Z.-F. Geological formation and geo-hazards during subway construction in Guangzhou. *Environ. Earth Sci.* **2016**, *75*, 934
27. Tan, Y.; Lu, Y.; Wang, D.L. Catastrophic failure of Shanghai metro line 4 in July 2003: Occurrence, emergency response, and disaster relief. *J. Perform. Constr. Facil.* **2021**, *35*, 04020125
28. Xie, H.; Zhu, J.; Zhou, T.; Zhang, K.; Zhou, C. Conceptualization and preliminary study of engineering disturbed rock dynamics. *Géoméch. Geophys. Geo-Energy Geo-Resour.* **2020**, *6*, 34. <https://doi.org/10.1007/s40948-020-00157-x>
29. Zhang, K.; Xie, H.; Guo, W.; Zhou, C.; Hu, G.; Luo, J.; Qiu, J.; Zhu, J. Experimental study on dynamic response of rock tunnel subjected to train moving load. *Géoméch. Geophys. Geo-Energy Geo-Resour.* **2023**, *9*, 125. <https://doi.org/10.1007/s40948-023-00666-5>
30. Qionglin, L.; Yulan, Q.; Kai, C.; Dongjie, Z.; Pangju, L. Review of Dynamic Behaviors and Constitutive Model of Soil Under Long-Term Cyclic Loading. *J. Southwest Jiaotong Univ.* **2024**, *59*, 377–391. <https://doi.org/10.3969/j.issn.0258-2724.20210928>
31. Cao, Z.; Sun, S.; Yuan, Z.; Cai, Y. Analytical Study on the Effect of Moving Surface Load on Underground Tunnel. In *Proceedings of China-Europe Conference on Geotechnical Engineering, Vienna, Austria, 13–16 August 2018*; Springer Series in Geomechanics and Geoengineering; Wu, W., Yu, H.S., Eds.; Springer: Cham, Switzerland, 2018. https://doi.org/10.1007/978-3-319-97115-5_163
32. Groundwater Dynamics in the Plain Areas of Beijing, Beijing Water Authority. Available online: https://swj.beijing.gov.cn/swdt/tzgg/202402/t20240222_3567361.html (accessed on 17 April 2024).
33. Watts, G.; Krylov, V. Ground-borne vibration generated by vehicles crossing road humps and speed control cushions. *Appl. Acoust.* **2000**, *59*, 221–236.
34. *Huang Yangxian Road Analysis and Design*; People's Transportation Press: Beijing, China, 1998
35. Chaoyang, X.; Feng, Z.; Hui, L. Research on the bearing characteristics and mechanisms of pile supported embankments under dynamic loads. *Geotech. Mech.* **2014**, *35*, 3231–3239 (In Chinese)
36. Fei, T.; Jinjing, C. Research on Traffic Load Characteristics and Simulation Methods. *J. Water Resour. Constr. Eng.* **2014**, *12*, 66–71 (In Chinese)
37. *JTGB 01-2014*; Highway Engineering Technical Standard. Ministry of Transport of People's Republic of China: Beijing, China, 2014. (In Chinese)

Disclaimer/Publisher's Note: The statements, opinions and data contained in all publications are solely those of the individual author(s) and contributor(s) and not of MDPI and/or the editor(s). MDPI and/or the editor(s) disclaim responsibility for any injury to people or property resulting from any ideas, methods, instructions or products referred to in the content.